Journal of Experimental Botany
doi:10.1093/jxb/eraa167 Advance Access Publication 3 April 2020
This paper is available online free of all access charges (see https://academic.oup.com/jxb/pages/openaccess for further details)

RESEARCH PAPER

Arabidopsis RAD23B regulates pollen development by mediating degradation of KRP1

Lan Li[1,†], Bin Li[1,†], Chong Xie[1], Teng Zhang[1], Cecilia Borassi[2], José M. Estevez [2,3,*], Xiushan Li[1,*] and Xuanming Liu[1,*]

[1] College of Biology, State Key Laboratory of Chemo/Biosensing and Chemometrics and Hunan Key Laboratory of Plant Functional Genomics and Developmental Regulation Hunan University, Changsha 410082, P. R. China
[2] Fundación Instituto Leloir and IIBBA-CONICET, Av. Patricias Argentinas 435, Buenos Aires CP C1405BWE, Argentina
[3] Centro de Biotecnología Vegetal, Facultad de Ciencias de la Vida, Universidad Andres Bello, Santiago, 8370186, Chile and Millennium Institute for Integrative Biology (iBio), Santiago, 8331150, Chile

[†] These authors contributed equally to this work.
* Correspondence: xmL05@hnu.edu.cn, lxs812_88@163.com, jestevez@leloir.org.ar, or jose.estevez@unab.cl

Received 30 December 2019; Editorial decision 26 March 2020; Accepted 2 April 2020

Editor: Peter Bozhkov, Swedish University of Agricultural Sciences, Sweden

Abstract

The ubiquitin (Ub)/26S proteasome system (UPS) plays a key role in plant growth, development, and survival by directing the turnover of numerous regulatory proteins. In the UPS, the ubiquitin-like (UBL) and ubiquitin-associated (UBA) domains function as hubs for ubiquitin-mediated protein degradation. Radiation sensitive 23 (RAD23), which has been identified as a UBL/UBA protein, contributes to the progression of the cell cycle, stress responses, ER proteolysis, and DNA repair. Here, we report that pollen development is arrested at the microspore stage in a *rad23b* null mutant. We demonstrate that RAD23B can directly interact with KIP-related protein 1 (KRP1) through its UBL-UBA domains. In addition, plants overexpressing *KRP1* have defects in pollen development, which is a phenotype similar to the *rad23b* mutant. RAD23B promotes the degradation of KRP1 *in vivo*, which is accumulated following treatment with the proteasome inhibitor MG132. Our results indicate that RAD23B plays an important in pollen development by controlling the turnover of the key cell cycle protein, KRP1.

Keywords: Cell cycle, KRP1, pollen abortion, proteasome system, RAD23B, ubiquitin.

Introduction

In eukaryotes the ubiquitin (Ub)/26S proteasome system (UPS) controls protein degradation by orchestrated targeting, ubiquitin-labeling, and degradation of proteins. The UPS plays a vital role in many biological processes such as plant growth (Shen *et al.*, 2005), development (Kurepa *et al.*, 2009), and survival (Du *et al.*, 2009). Ubiquitin-like (UBL) and ubiquitin-associated (UBA) domains function as hubs during ubiquitin-mediated protein degradation (Lowe *et al.*, 2006). Although the importance of the UPS in substrate recognition is widely known, the function of UBL/UBA proteins in the plant kingdom remains elusive (Medina *et al.*, 2012). In animals, Radiation sensitive 23 (RAD23), which has been identified as a UBL/UBA protein, contains an amino-terminal UBL domain and two UBA domains (Andersson *et al.*, 2005). RAD23 plays an important role in the regulation of the cell cycle (Díaz-Martínez *et al.*, 2006), and knockout of RAD23

Abbreviations: CDK, cyclin-dependent kinase; DSK2, dominant suppressor of KAR2; ICK, interactors of Cdc2 kinase; KRP, kip-related protein; UBA, ubiquitin-associated; UBL, ubiquitin-like; UPS, ubiquitin-proteasome system.

has been shown to inhibit cell growth (Hänzelmann *et al.*, 2010). In plants, *rad23b* mutants display pleiotropic developmental defects, abnormal phyllotaxy, shorter primary roots, unfertilized ovules, smaller siliques, and have reduced seed set (Farmer *et al.*, 2010). It has also been reported that RAD23 regulates plant development, presumably by delivering target proteins to the UPS (Liang *et al.*, 2014).

The regulation mechanisms of the cell cycle, which can be divided into the four phases G1, S, G2, and M, are highly conserved (Cross *et al.*, 2011). It has been shown that there are two major cell-cycle checkpoints, the transition G1 phase prior to the initiation of the S phase (G1–S transcription) and the transition from the G2 phase into the M phase (G2–M transcription) (Haase and Wittenberg, 2014). Cellular cyclin-dependent kinases (CDKs) are important in cell-cycle progression and cell division (Ding *et al.*, 2005). CDK inhibitors (interactors of Cdc2 kinases, ICKs) can affect activity through direct protein binding. To date, seven ICKs have been identified in Arabidopsis (De Veylder *et al.*, 2001; Bird *et al.*, 2007). Among them, the transcript levels of *KRP1* and *KRP2* are significantly regulated by Protein arginine methyltransferase 5 (PRMT5) during shoot regeneration (Liu *et al.*, 2016). Moreover, ICK1/KRP1 and ICK2/KRP2 have been observed to be regulated by the 26S proteasome (Weinl *et al.*, 2005; Lai *et al.*, 2009). KRP1 degradation is dependent on both SCF ^{SKP2b} and the RING protein RPK (Ren *et al.*, 2008). However, how KRPs are degraded remains unknown.

In this study, we found that the incidence of abnormal microspore development increased in the *rad23b* mutant, and this phenotype was similar to that of KRP1-overexpression plants. Furthermore, yeast two-hybrid assays demonstrated that RAD23B directly interacted with KRP1. In addition, we also found that RAD23B promoted the degradation of KRP1 *in vivo*. These results indicated that the interaction of RAD23B and KRP1 is essential for the degradation of KRP1 and the regulation of cell division. We therefore conclude that RAD23B controls cell division by promoting the degradation of KRPs in pollen grains.

Materials and methods

Plant material and growth conditions

All the Arabidopsis mutants used in this study were derived from the Col-0 background. The *rad23b-1* (Salk_075940) and *rad23b-2* (Salk_130110) mutants were obtained from the ABRC (https://abrc.osu.edu/). The T-DNA insertion mutants were identified by PCR using the primers LP and RP (Supplementary Table S1 at *JXB* online). The T-DNA insertion site, as described at http://signal.salk.edu, was confirmed by PCR-based genotyping (Peng *et al.*, 2012; Zhang *et al.*, 2012*a*). Arabidopsis seeds were stratified at 4 °C for 2 d before being grown for subsequent analysis on half-strength Murashige and Skoog medium with 0.8% sucrose and 1% Phytagel (A7002, Sigma-Aldrich). All plants were grown under a 16/8h light/dark cycle at 22 °C with 60 μmol m^{-2} s^{-1}.

Construction of transgenic plants

Fragments of *RAD23B* were amplified and cloned into the entry vector pDONR201 using a Gateway strategy. The coding sequence of *RAD23B* was then cloned into the destination vector *pENSG-GFP-GW*. In addition, *RAD23B* and *KRP1* were also cloned into the vector pDT1 using the primers *RAD23B-pDT1-F*, *RAD23B-pDT1-R*, *KRP1-pDT1-F*, and *KRP1-pDT1-R*, respectively. All of the resulting plasmids were used to transform *Agrobacterium tumefaciens* GV3101 by electroporation for delivery into Arabidopsis Col-0. The *rad23-b* mutant plants were created using the floral dip method (Clough and Bent, 1998). The transgenic plants were screened using the herbicide Basta to identify homozygous lines. Leaves and flowers from the homozygous transgenic lines were sampled and stored at −80 °C. All the primers used are detailed in Supplementary Table S1.

Extraction of total RNA and RT-PCR analysis

Six randomly selected 7-d-old seedlings were sampled. Total RNA was isolated as described previously (Peng *et al.*, 2012), and reverse-transcribed to cDNA using a PrimeScript RT Reagent Kit with gDNA Eraser (Takara) after DNase treatment. The cDNA product was diluted 20-fold, and 0.5 μl was then used in a 20-μl PCR reaction. The expression level of *KRP1* was measured by quantitative real-time PCR for at least three independent experiments (n=3). The sequences of the RT-PCR-rad23b-1 and RT-PCR-rad23b-2 primers used in this study are listed in Supplementary Table S1.

GUS staining analysis

Fragments of the *RAD23B* promoter (−1449 to +826 bp from the translation start site) were amplified from genomic DNA by PCR using the primers *RAD23B-p*R and *RAD23B-p*F (Supplementary Table S1). The fragments were then sub-cloned into the empty vector pDONR207 using BP Clonase for downstream sequencing analysis. Positive fragments were cloned into the destination vector *GW-GUS* using LR Clonase, and were then transformed into *A. tumefaciens* GV3101 by electroporation for gene delivery into the Arabidopsis plants using the floral dip method. The transgenic plants were screened using the herbicide Basta to identify homozygous transgenic lines. Tissues from the homozygous plants were stained with GUS (β-glucuronidase) stain solution as previously described (Jefferson *et al.*, 1986) and images were taken under a dissecting microscope.

Hematoxylin staining

Paraffin cross-sectioned samples were examined using hematoxylin as described previously (Fischer *et al.*, 2008). The sections were dewaxed and incubated with 10% H_2O_2 for 10 min and the slides were then dipped into a Coplin jar containing Mayer's hematoxylin and agitated for 30 s. The sections were dehydrated with two changes of 95% alcohol and examined using a TE2000 electron microscope (Nikon).

In vitro pollen germination analysis

Pollen germination analysis was performed following the method of Fan *et al.* (2001). Fifty flowers were randomly sampled from different mutant and wild-type plants. The anthers were carefully placed in 1.5-ml microtubes or Eppendorf microtubes with 700 μl of liquid germination medium (GM), oscillated for 2–3 min, transferred to a new microtube, and collected using centrifugation at 12 000 *g* for 2 min. Pollen grains were resuspended in liquid GM and cultured in semi-solid GM supplemented with 0.5% agarose in a chamber at 23 °C with 100% relative humidity. After 8 h incubation the germinated pollen grains were counted under the Nikon TE2000 microscope. Data are presented as the means of three independent experiments, in each of which 150–200 grains were counted.

Yeast two-hybrid assays

Yeast two-hybrid (Y2H) was assays were performed as described previously (Du *et al.*, 2016). Briefly, the full length of *RAD23-B* was amplified using primers (Supplementary Table S1) and sub-cloned in-frame with GAL4D-AD (pGADT7) as a bait. The *KRP1* coding sequence was inserted into GAL4D-BD (pGBKT7) as a prey in the same manner. The

bait and prey vectors were transfected into the yeast strain AH109 to create the GAL4-based Y2H system. Colonies were selected and grown in the absence of histidine, but in the presence of 10 mM 3-AT (Sigma), and images were taken after 5–7 d.

In vitro GST pull-down analysis

A glutathione S-transferase (GST) pull-down assay was conducted as previously described (Du *et al.*, 2016), with minor modifications. The coding sequence of *RAD23B* was cloned into the pGEX4T-1 vector, and the coding sequences of *KRP*s were sub-cloned into the pET28b vector. The specific primers used are given in Supplementary Table S1. Seven purified His-KRPs were each incubated with either GST protein or GST-RAD23B protein using Glutathione Agarose (40 µl, ThermoFisher Scientific) at 4 °C for 2 h, with a 5% mixture of each being used for input. The Glutathione Agarose was washed five times with PBS and bound proteins were eluted from with 40 µl of elution buffer (50 mM Tris-Cl, 300 mM NaCl, 20 mM reduced glutathione, pH 8). The resulting isolated proteins were detected by immunoblot analysis using anti-His and anti-GST antibodies as primary antibodies.

Bimolecular fluorescence complementation assays

For bimolecular fluorescence complementation (BiFC) assays, the coding sequence of *RAD23B* was cloned into the pE3308 vector, and the coding sequence of *KRP1* was sub-cloned into the pE3449 vector. The primers for cloning are given in Supplementary Table S1. The constructed plasmids were co-transfected into protoplasts, which were isolated from 4-week-old Arabidopsis rosette leaves through cellulase and macerozyme digestion. The transformation method was performed as described previously by Li *et al.* (2018), and the co-transfected protoplasts were incubated in the dark at 22 °C for 18 h to allow for the expression of the BiFC proteins. Fluorescence was detected using an A1R SI confocal laser-scanning microscope (Nikon), with wavelengths of 488 nm for GFP.

Alexander's and DAPI staining

Pollen grains were treated with DAPI (4′,6-diamidino-2-phenylindole) or Alexander's stain to monitor their development (Alexander, 1969; Park *et al.*, 1998). Briefly, the grains were separated from stamens and stained for 30 min using Alexander's solution (10% alcohol, 25% glycerol, 4% glacial acetic acid, 500 mg ml^{-1} phenol, 500 mg ml^{-1} chloral hydrate, 0.5 mg ml^{-1} acid fuchsin, and 0.05 mg orange G), and then examined under a microscope. In addition, grains were incubated in the dark for 5 min with DAPI staining solution (0.1 M sodium phosphate, 1 mM EDTA, 0.1% Triton X-100, 0.4 µg ml^{-1} DAPI, pH 7; Sigma) and then examined using fluorescence microscopy.

Detection of protein degradation in vivo

Plants were grown on half-strength MS medium for 7 d and then samples were treated with 40 µM of the proteasome inhibitor MG132 for 12 h. Total protein was extracted using NEB-T buffer (50 mM HEPES, 40 mM KCl, 5 mM $MgCl_2$, and 1% Triton X-100, pH7.5). The extracts were centrifuged at 12 000 *g* for 20 min at 4 °C, and the supernatants were examined by western blot analysis. Protein bands were detected by immunoblot analysis using anti-Myc and anti-β-actin antibodies as primary antibodies.

Results

RAD23B *is involved in the regulation of pollen grain development*

To study the expression pattern of *RAD23B*, a construct with a GUS reporter gene driven by the *RAD23B* promoter was introduced in wild-type Col-0 plants (Fig. 1A). We randomly selected seven of the transgenic lines for *RAD23B* expression pattern analysis and found that the GUS signal could clearly be detected in the young leaves (Fig. 1B) and especially in the anthers, and specifically in pollen grains (Fig. 1C). In contrast, the GUS signals in the petals, sepals, and pistil tissues were weak or undetectable (Fig. 1D). To examine the biological function of *RAD23B*, knockout lines for homozygous T-DNA insert mutants obtained from ABRC were first identified by PCR (Fig. 2A, B) and further confirmed by semi-quantitative RT-PCR. Compared to the Col-0 wild-type (WT), the expression of *RAD23B* was not detectable in the two T-DNA mutants (Fig. 2C), indicating that the T-DNA insertions did indeed disrupt the expression of *RAD23B*, and that *rad23b-1* and *rad23b-2* were both null mutants. To obtain *RAD23B*-overexpression lines, WT plants were transformed with the full-length *RAD23B* coding sequence driven by the CaMV35S promoter (Col-0/*35S::RAD23B-Myc*). Two positive transgenic lines were confirmed by western blotting and showed high expression levels of RAD23B (Fig. 2D). In addition, the *rad23b-1* mutant was transformed with the same overexpression construct (*rad23b-1/35S::RAD23B-Myc*) and positive plants were selected for subsequent experiments. Since *RAD23B* was expressed in pollen grains, its role in the regulation of the cell cycle was followed in grains at different developmental stages using hematoxylin staining (Fischer *et al.*, 2008). We found that the microspores of the *rad23b-1* mutant at the G1–S transcription displayed no detectable defects, but they became much more vacuolated than the WT at the binuclear cell stage (Fig. 2E). At the G2–M transcription, the *rad23b-1* mutant showed an increased number of microspore vacuolizations. Overexpression of *RAD23B* (*rad23b-1/35S::RAD23B-Myc*) was capable of completely rescuing the vacuolization defects in the *rad23b-1* mutant plants (Fig. 2E). Taken together, the results suggest that *RAD23B* plays an important role in the regulation of the cell cycle inpollen grains. We also investigated pollen germination rates in the WT, the *rad23b-1* mutant, Col-0/*35S::RAD23B*, and *rad23b-1/35S::RAD23B* plants and found that they were 91.7%, 61.6%, 91.4%, and 91.9%, respectively (Supplementary Fig. S1). The germination rate of the *rad23b-1* mutant was significantly lower than that of the WT. More importantly, *rad23b-1/35S::RAD23B* was able to fully rescue the pollen germination phenotype, which strongly suggested that the absence of RAB23B was the cause of this developmental phenotype.

RAD23B interacts with the CDK inhibitor KRP1 through its UBL-UBA domain

To better understand the function of RAD23B, Y2H assays were used to screen interacting proteins (Du *et al.*, 2016). One cyclin-dependent kinase inhibitor, KRP1, was observed to interact with RAD23B. To further confirm this interaction, an *in vitro* pull-down assay was used to investigate the interaction of RAD23B with KRPs. Seven His-KRPs and GST-RAD23B fusion proteins were expressed and purified (Supplementary Fig. S2). We found KRP1 strongly interacted with RAD23B, whilst KRP6 (another cyclin-dependent kinase inhibitor) also interacted but only weakly (Fig. 3A). The constructs were

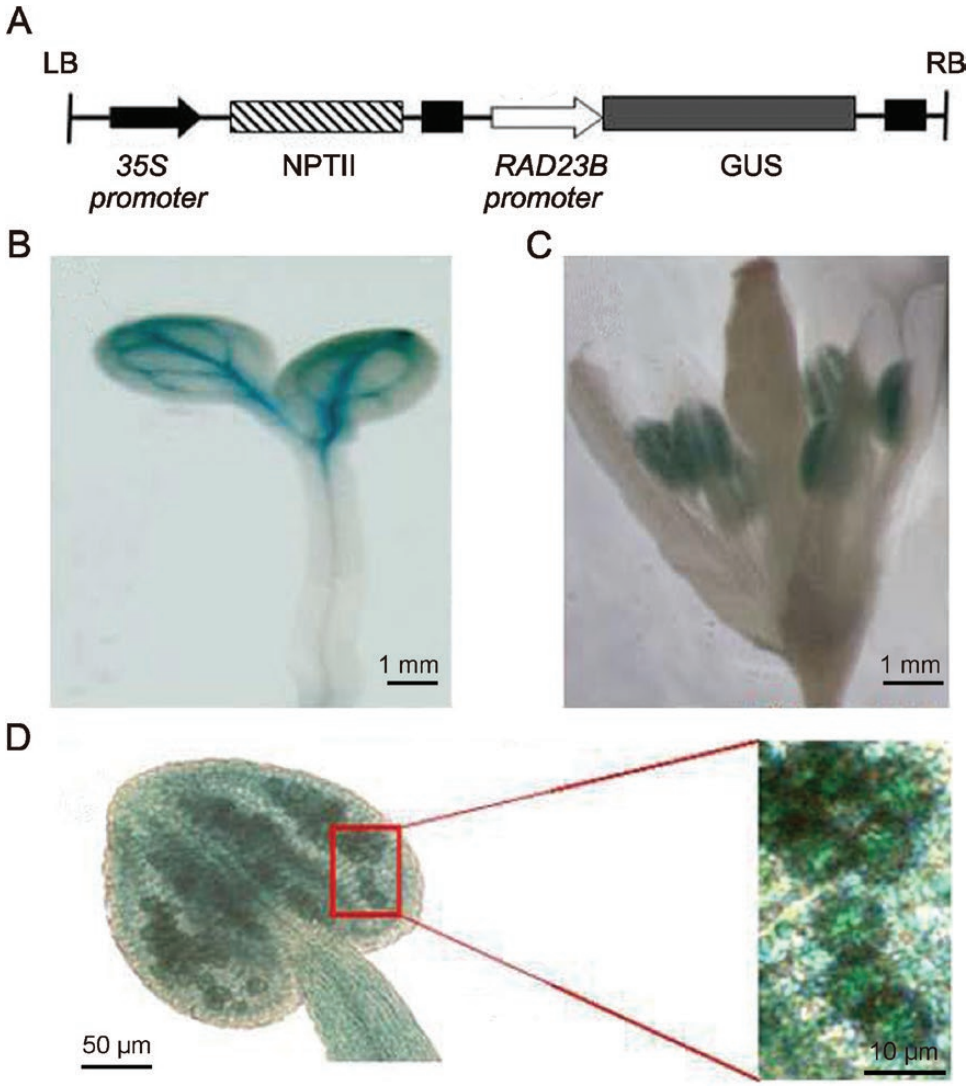

Fig. 1. Expression patterns of *RAD23B* in Arabidopsis plants. (A) Schematic diagram of the construct for GUS staining. (B–D) GUS staining of (B) developing leaves of 6-d-old plantlets, (C) flower organs of 42-d-old plants, and (D) the pollen grains shown in (C).

then co-transformed into AH109 yeast cells and selected on synthetic dropout medium to test the interaction. In addition, full-length coding sequences of RAD23B and KRP1 were cloned into the vector pairs GAL4D-AD (pGADT7) and GAL4D-BD (pGBKT7) to generate AD-RAD23B and BD-KRP1. A strong interaction was observed as only the cells that co-expressed RAD23B and KRP1 could grow in medium without His (Fig. 3B). To confirm the *in vivo* interaction, we used BiFC assays. Green fluorescent protein (GFP) signal could be detected when RAD23B-nVenus and KRP1-CFP were co-expressed (Fig. 3C). These data reinforced the conclusion that RAD23B physically interacts with KRP1 *in vitro* and *in vivo*. To investigate which domains contributed to the interaction, RAD23B-L (lacking any UBL domains), RAD23B-U (lacking one UBA domain), RAD23B-US (lacking one UBA domain and the STI1 domain), and RAD23B-USU (lacking any UBA domains and the STI1 domain) were cloned into the GAL4D-AD (pGADT7) vector and transformed into AH109 yeast cells to test the interaction with KRP1 (Fig. 3D). Full-length RAD23B was used as a positive control. We found that KRP1 interacted with RAD23B only when both the UBL and UBA domains of RAD23B were present, which indicated that the UBL-UBA domains of RAD23B are essential for the interaction.

RAD23B contributes to KRP1 degradation through 26S proteasome-dependent proteolysis

RAD23B, functions as a hub during ubiquitin-mediated protein degradation (Bergink *et al.*, 2013). Having found that it could directly interact with KRP1, we hypothesized that RAD23B may contribute to KRP1 degradation. To test this, we measured the protein levels of in the WT and in the *rad23b-1* mutant, and found that KRP1 significantly increased in the absence of RAD23B in the mutant (Fig. 4A). To exclude the possibility that this increase was due to deregulation of transcripts, we examined the gene expression levels of *KRP1*. There were no significant differences between the WT and the *rad23b-1* mutant (Fig. 4B). Furthermore, the accumulation of the KRP1 protein in the

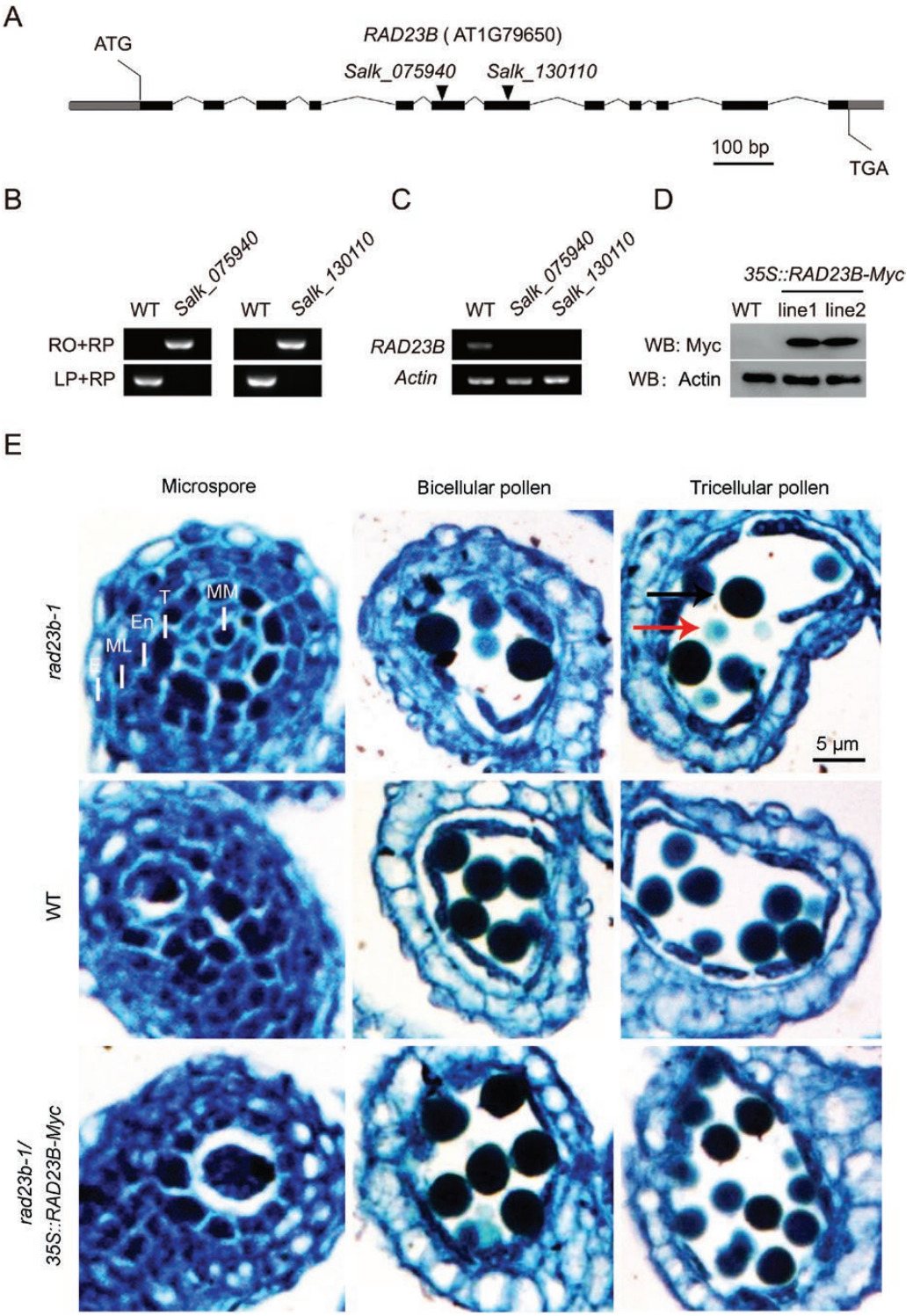

Fig. 2. Lack of RAD23B induces abortion of pollen grains in Arabidopsis. (A) Schematic diagram of the gene structure of *RAD23B*, including the locations of the T-DNA insertions in the two mutant lines SALK_075940 (*rad23b-1*) and SALK_130110 (*rad23b-2*). (B) PCR identification of homozygous lines of the T-DNA mutants using various primer combinations. The presence and absence of the T-DNA insertions correspond to the PCR products from the primers R0+RP and LP+RP, respectively. WT, wild-type (Col-0). (C) Expression of RAD23B in the WT and the two mutant lines. *Actin2* served as an internal control. (D) Western blotting analysis of the WT and two transgenic lines of Col-0/*35S::RAD23B*. β-Actin was used as a loading control. (E) Transverse sections of flowers stained with hematoxylin as examined by light microscopy. Red arrows indicate abortive microspores, and black arrows indicate normal microspores. E, epidermis; En, endothecium; ML, middle layer; T, tapetum; MM, microspore mother cell.

WT could be mimicked in the mutant as a result of treatment with the proteasome inhibitor MG132 (Fig. 4C), while the gene expression level of *KRP1* remain unaltered (Fig. 4D). Taken together, our results showed that the intracellular level of KRP1 was regulated by RAD23B through 26S proteasome-dependent proteolysis.

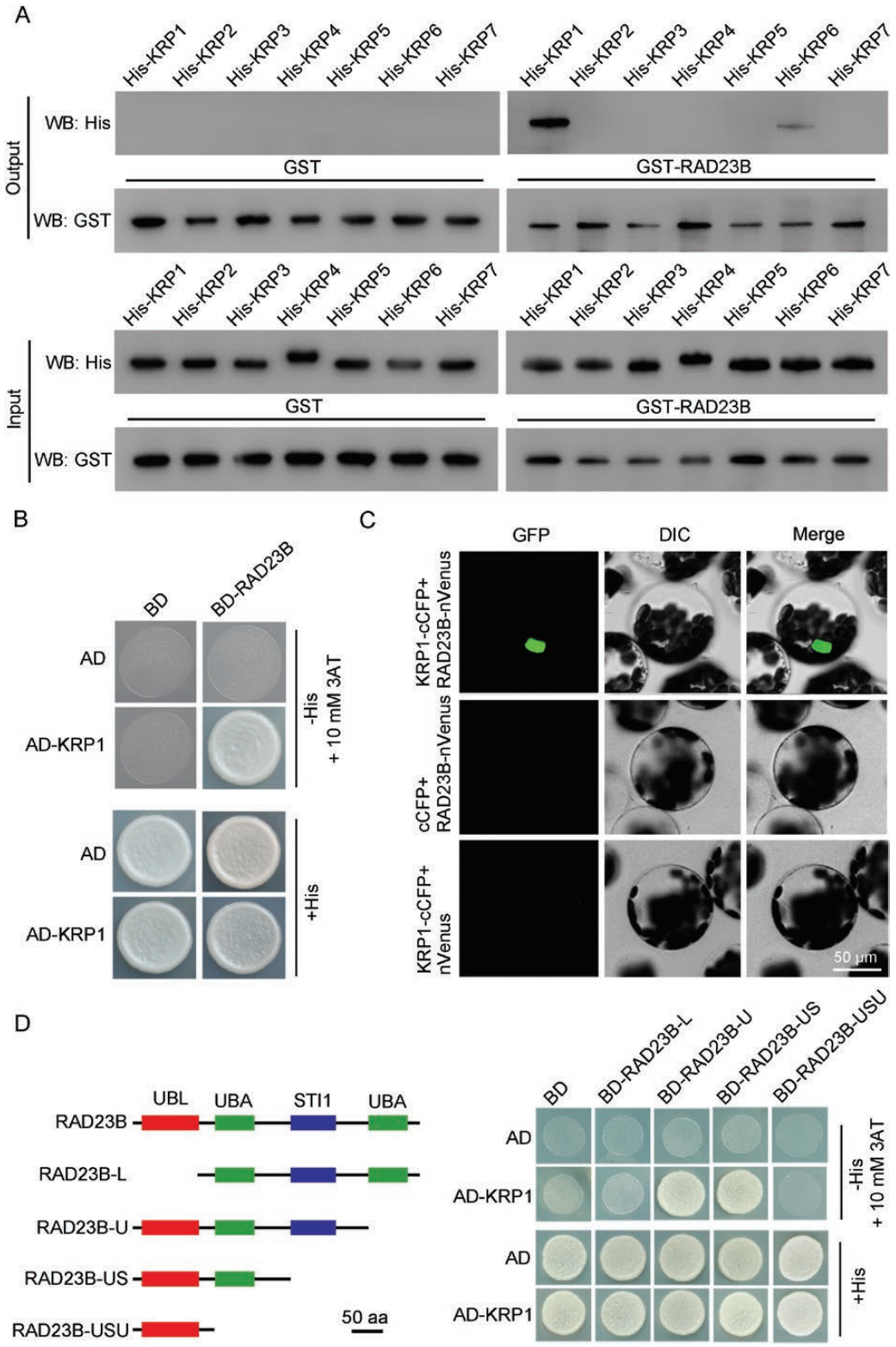

Fig. 3. UBL-UBA domains are required for the interaction of RAD23B with KRP1. (A) Pull-down assays of RAD23B-GST and His-KRPs. The complex was separated using SDS-PAGE and tested using anti-His (top) and anti-GST (bottom) primary antibodies. (B) Yeast two-hybrid (Y2H) assays to examine the interaction between KRP1 and RAD23B on SDIII agar medium (–Trp, –Leu, –His, +10 mM 3AT). (C) RAD23B-cCFP and KRP1-nVenus were co-expressed in mesophyll protoplasts of Arabidopsis. GFP fluorescence was detected in the protoplasts of RAD23B-cCFP+KRP1-nVenus, but not in the control. All experiments were repeated three times and representative images are shown. DIC, differential interference contrast. (D) Y2H assays to examine the interactions between KRP1 and four different domain combinations of RAD23B (full length), RAD23B-L (74–395 amino acids), RAD23B-U (1–217), RAD23B-US (1–115), and RAD23B-USU (1–74).

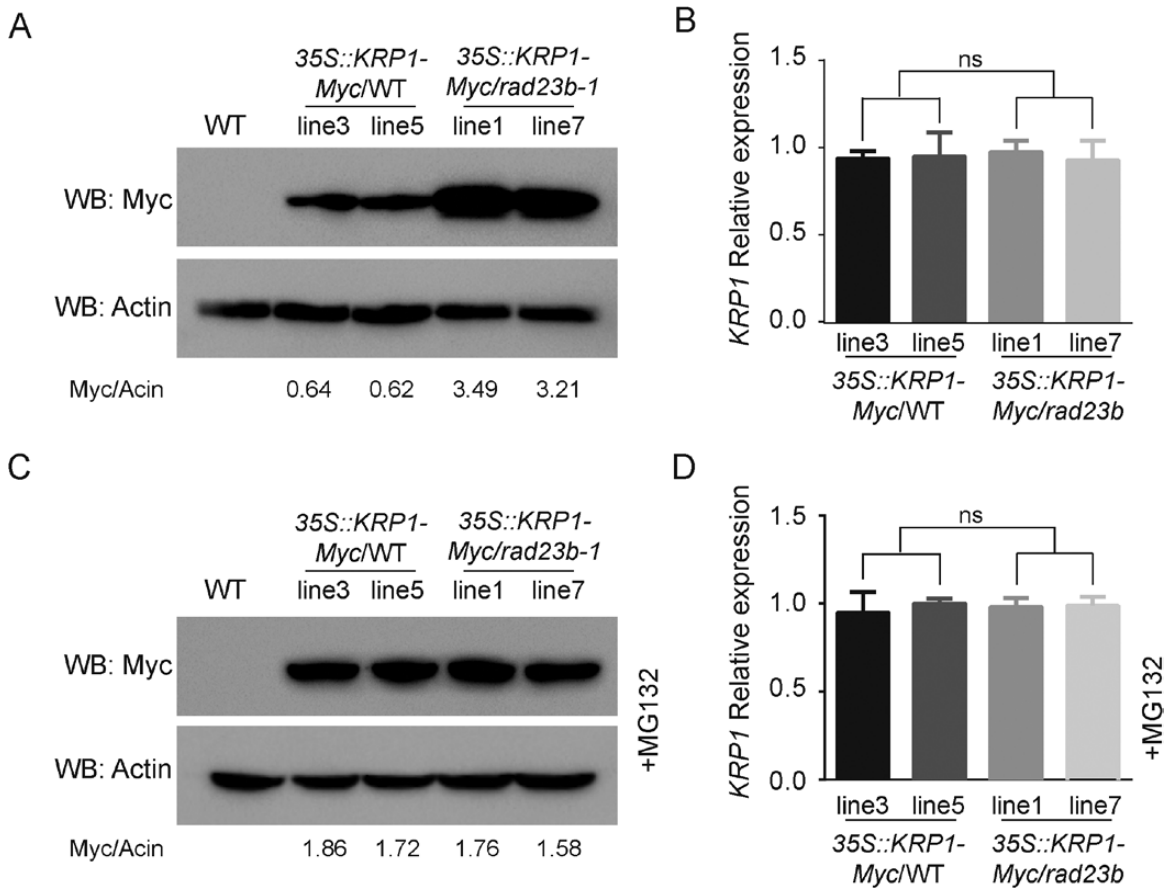

Fig. 4. Effects of RAD23B on the degradation of KRP1 in Arabidopsis *in vivo*. (A) Immunoblots showing KRP1 levels in the presence or absence of RAD23B and in the Col-0 wild-type (WT, negative control). Results from two lines of each transgenic plants are shown. Actin was used as the loading control, and the ratio of Myc/Actin is shown below the gel. (B) Relative expression of *KRP1* in *35S::KRP1-Myc* T2 transgenic plants in the WT (lines 3 and 5) and in the *rad23b-1* background (lines 1 and 7). Gene expression was determined by quantitative real-time PCR and was normalized against the expression of *Actin*. Data are means (±SD), *n*=3. ns, not significant. (C) Immunoblots showing KRP1 levels in the presence or absence of RAD23B under treatment with the proteasome inhibitor MG132. The ratio of Myc/Actin is shown below the gel. (D) Relative expression of *KRP1* in the plants shown in (C) treated with MG132. Gene expression was determined by quantitative real-time PCR and was normalized against the expression of *Actin*. Data are means (±SD), *n*=3. ns, not significant.

Overexpression of KRP1 mimics the phenotype of rad23b *mutant plants*

Our results showed that the *rad23b-1* mutant was defective in pollen development and that RAD23B could directly interact with KRP1, and therefore it was reasonable to suspect that KRP1 was also involved in regulation of pollen development. Two independent lines of *KRP1*-overexpression transgenic plants (*35S::KRP1-Myc*) were confirmed by western blotting (Fig. 5A). For further analysis, we used *35S::KRP1-Myc* line-2 as it showed the highest protein level. Male gametogenesis was examined for Col-0/*35S::KRP1-Myc-2*, Col-0, and *rad23b-1* plants using DAPI and Alexander's staining (Alexander, 1969; Park *et al.*, 1998), and we found that the microspores of *rad23b-1* and Col-0/*35S::KRP1-Myc-2* showed no differences compared to the WT at the G1–S transition stage (Supplementary Fig. S3). During the G2–M transition, both the *rad23b-1* mutant and Col-0/*35S::KRP1-Myc-2* had more microspore vacuolization than the WT (Fig. 5B). The vacuolization rates of the WT, *rad23b* mutant, and Col-0/*35S::KRP1-Myc-2* lines were 0.3%, 13.4%, and 16.8% , respectively, at the bicellular stage, and 0.3%, 50.6%, and 60.3%, respectively, at the tricellular stage (Fig. 5C). These results showed that the overexpression of *KRP1* could mimic the phenotype of the *rad23b-1* mutant, suggesting that both *KRP1* and *RAD23B* play an important role in cell division during pollen grain development.

Discussion

In eukaryotes, protein ubiquitination and degradation play critical roles in the control of the cell cycle by destroying important regulatory molecules (Liu *et al.*, 2008; Cross *et al.*, 2011). Among the various identified interactors of Cdc2 kinase (ICKs), proteins of the UBL/UBA family are believed to target and deliver poly-ubiquitin substrates to the proteasome, including RPN1, RPN10, and RPN13 (Brukhin *et al.*, 2005; Isasa *et al.*, 2010; Besche *et al.*, 2014; Hamazaki *et al.*, 2015), as well as RAD23 and DSK2,. Here, we have demonstrated that RAD23, also a member of UBL/UBA family, increased the degradation of KRP1 during the cell cycle G2–M transition via a direct interaction. In addition, genetic analysis suggested that the *rad23b* null mutant exhibited a similar phenotype to *KRP1*-overexpression plants. Taken together, these results

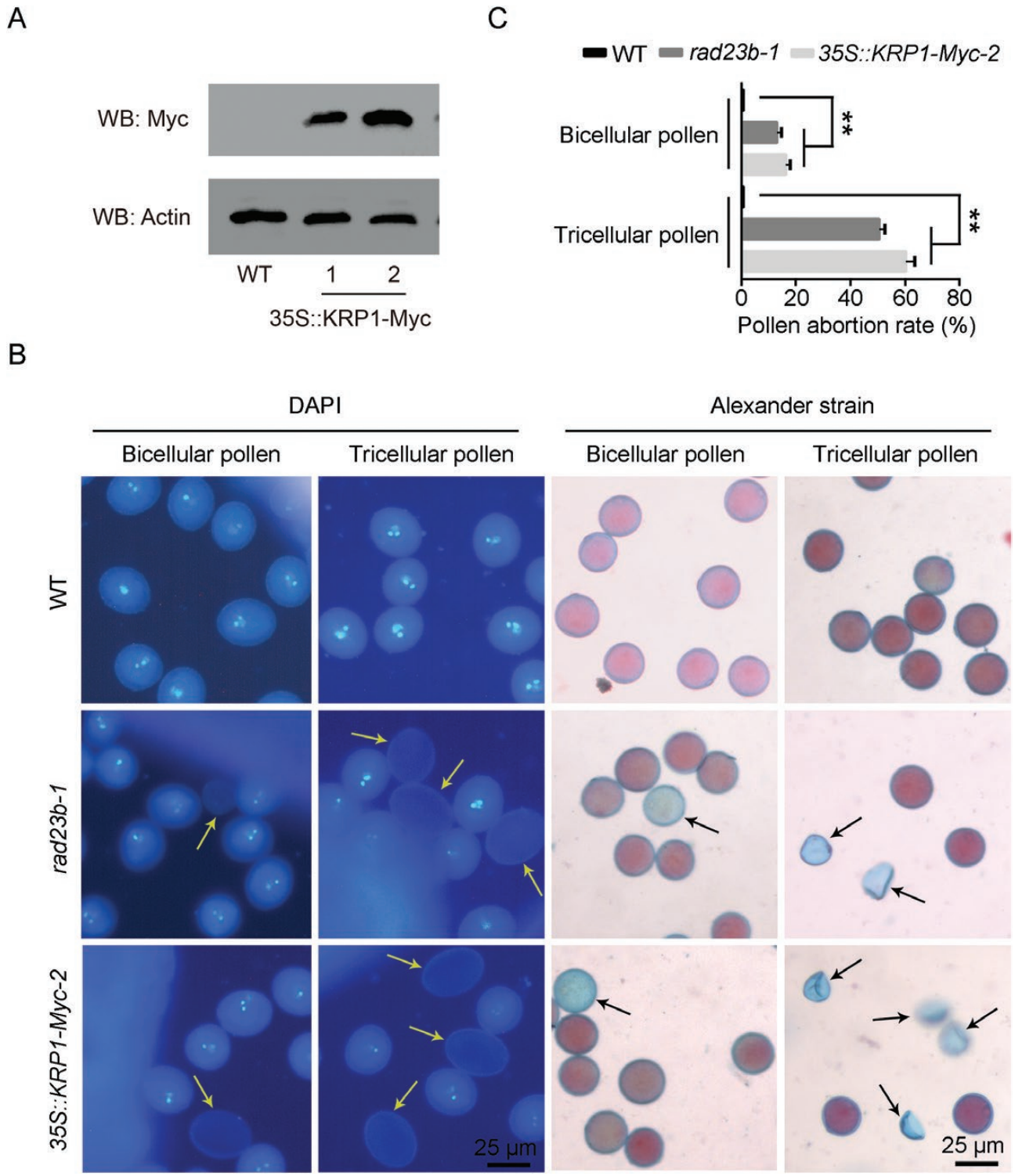

Fig. 5. Overexpression of KRP1 in Arabidopsis causes similar pollen defects to those observed in *rad23b* mutants. (A) Western blotting of two Col-0/*35S::KRP1-Myc-3* transgenic lines compared with the Col-0 wild-type (WT, negative control). (B) DAPI and Alexander's staining of the WT, *rad23b*, and Col-0/*35S::KRP1-Myc* pollen grains at the bicellular and tricellular stages. Yellow arrows indicate abnormal pollen grains with no DAPI staining, and the black arrows indicate shrunken pollen grains. (C) Pollen abortion rates. Data are means (±SD) of three independent experiments each of which included n=100 pollen grains. Significant differences compared with the WT were determined using Student's t-test: $^{**}P<0.01$.

provide compelling evidence that RAD23B is involved in the regulation of KRP1 and, accordingly, that it affects the regulation of the cell cycle.

Similar to other eukaryotes, plants express many UBL/UBA proteins, which are orthologous to yeast proteins such as RAD23, DSK2, and DDI1 (Díaz-Martínez *et al.*, 2006). The proteins possess similar structures, namely an N-terminal UBL domain and one or more C-terminal UBA domains (Liang *et al.*, 2014). UBL/UBA proteins are also likely to participate in many developmental events in plants, including regulation of the cell

cycle, DNA repair, and regulation of transcription (Mueller and Smerdon, 1996; Renaud *et al.*, 2011; Zhang *et al.*, 2012*b*). Recent studies have indicated that RAD23 binds some ubiquitin (Ub) conjugates, particularly through directly interacting with the 26S proteasome Ub-receptor RPN10, and that it is involved in protein degradation (Smalle *et al.*, 2003). It has also been reported that *rad23b* mutants exhibit a marked seed-abortion phenotype (Farmer *et al.*, 2010). Earlier studies had demonstrated that a *KRP1*-overexpression line displays shorter siliques and fertility defects, which is similar to the phenotype of *rad23b* mutants (Ren *et al.*, 2008), and (Farmer *et al.* (2010) speculated that RAD23 might promote the degradation of one or more cell-cycle proteins in order to regulate plant development. Here, we demonstrated that RAD23B was highly expressed in the young leaves (Fig. 1B), anthers, and pollen grains (Fig. 1C). In addition, knockout lines of RAD23B showed pronounced pollen abortion during the tricellular pollen stage, and this phenotype could be rescued by overexpression of RAD23B-Myc (Fig. 2E). Taken together, these data indicated that RAD23B was likely to be involved in the regulation of the cell cycle.

In yeast and animals, the SCF complex is a critical component for the regulation of cell division. The complex targets ICKs to the proteasome for degradation (Patton *et al.*, 1998). It has also been reported that CDKA;1/CYCD2;1 plays a critical role in the G1–S transition (Churchman *et al.*, 2006; Hirano *et al.*, 2011). Furthermore, KRP1 has been demonstrated to interact directly with CDKA;1/CYCD2;1 *in vivo* (Cheng *et al.*, 2015; Vieira *et al.*, 2017), which strongly suggests that it has crucial functions in the regulation of the G1–S transition. Interestingly, Weinl *et al.* (2005) reported that KRP1 also plays an important role in the G2–M transition to regulate the entry into mitosis, although a detailed understanding of the mechanisms is lacking. Here, we demonstrated that RAD23B interacted directly with KRP1 *in vivo* and *in vitro* (Fig. 3) and that the *rad23b* mutants exhibited an increased frequency of abnormal microspores during the G2–M transition phase (Fig. 2). Similarly, this phenotype could also be observed in the *KRP1*-overexpression line (Fig. 5). In addition, genetic evidence indicated that RAD23B also contributed to the degradation of KRP1, and thus the latter was more stable in the *rad23b* mutant. Accumulation of the KRP1 protein in the wild-type following treatment with the proteasome inhibitor MG132 suggested that RAD23 mediated its degradation through trafficking of the substrates to the proteasome. Taken together, our data indicate that RAD23B functions as a negative regulator of KRP1 to modulate cellular division during pollen grain development.

Supplementary data

Supplementary data are available at *JXB* online.

Fig. S1. Phenotype analysis of pollen grain germination in the different genotypes.

Fig. S2. Protein purification of GST-RAD23B and His-KRPs.

Fig. S3. Comparison of pollen grains from the wild-type, *rad23b-1*, and *35::KRP1-Myc* at the G1–S transition stage.

Table S1. List of primers used in this study.

Acknowledgements

This research was financially supported by the National Science Foundation of China (Nos. 31571635, 31871595), the Hunan Provincial Important Science and Technology Specific Projects (No. 2018NK1010), and the Planned Science and Technology Project of Changsha City (No. kq1801001). This work was also supported by grants from ANPCyT (PICT2016-0132 and PICT2017-0066), ICGEB (CRP/ARG16-03), and Instituto Milenio iBio – Iniciativa Científica Milenio, MINECON to JME.

References

Alexander MP. 1969. Differential staining of aborted and nonaborted pollen. Stain Technology **44**, 117–122.

Andersson HA, Passeri MF, Barry MA. 2005. Rad23 as a reciprocal agent for stimulating or repressing immune responses. Human Gene Therapy **16**, 634–641.

Bergink S, Theil AF, Toussaint W, *et al*. 2013. Erythropoietic defect associated with reduced cell proliferation in mice lacking the 26S proteasome shuttling factor Rad23b. Molecular and Cellular Biology **33**, 3879–3892.

Besche HC, Sha Z, Kukushkin NV, *et al*. 2014. Autoubiquitination of the 26S proteasome on Rpn13 regulates breakdown of ubiquitin conjugates. The EMBO Journal **33**, 1159–1176.

Bird DA, Buruiana MM, Zhou Y, Fowke LC, Wang H. 2007. *Arabidopsis* cyclin-dependent kinase inhibitors are nuclear-localized and show different localization patterns within the nucleoplasm. Plant Cell Reports **26**, 861–872.

Brukhin V, Gheyselinck J, Gagliardini V, Genschik P, Grossniklaus U. 2005. The RPN1 subunit of the 26S proteasome in *Arabidopsis* is essential for embryogenesis. The Plant Cell **17**, 2723–2737.

Cheng Y, Liu H, Cao L, Wang S, Li Y, Zhang Y, Jiang W, Zhou Y, Wang H. 2015. Down-regulation of multiple CDK inhibitor ICK/KRP genes promotes cell proliferation, callus induction and plant regeneration in *Arabidopsis*. Frontiers in Plant Science **6**, 825.

Churchman ML, Brown ML, Kato N, *et al*. 2006. SIAMESE, a plant-specific cell cycle regulator, controls endoreplication onset in *Arabidopsis thaliana*. The Plant Cell **18**, 3145–3157.

Clough SJ, Bent AF. 1998. Floral dip: a simplified method for *Agrobacterium*-mediated transformation of *Arabidopsis thaliana*. The Plant Journal **16**, 735–743.

Cross FR, Buchler NE, Skotheim JM. 2011. Evolution of networks and sequences in eukaryotic cell cycle control. Philosophical Transactions of the Royal Society of London. Series B, Biological Sciences **366**, 3532–3544.

De Veylder L, Beeckman T, Beemster GT, Krols L, Terras F, Landrieu I, van der Schueren E, Maes S, Naudts M, Inzé D. 2001. Functional analysis of cyclin-dependent kinase inhibitors of *Arabidopsis*. The Plant Cell **13**, 1653–1668.

Díaz-Martínez LA, Kang Y, Walters KJ, Clarke DJ. 2006. Yeast UBL-UBA proteins have partially redundant functions in cell cycle control. Cell Division **1**, 28–39.

Ding QJ, Jiang N, Chu XJ, *et al*. 2005. Design, synthesis of 1,4-cyclohexyldiamine substituted diaminopyrimidines as selective inhibitors of CDK1, CDK2 and CDK4 and their *in vitro* and *in vivo* evaluation. Cancer Research **46**, 4414.

Du C, Li X, Chen J, *et al*. 2016. Receptor kinase complex transmits RALF peptide signal to inhibit root growth in *Arabidopsis*. Proceedings of the National Academy of Sciences, USA **113**, E8326–E8334.

Du Z, Zhou X, Li L, Su Z. 2009. plantsUPS: a database of plants' Ubiquitin Proteasome System. BMC Genomics **10**, 227–233.

Fan LM, Wang YF, Wang H, Wu WH. 2001. *In vitro Arabidopsis* pollen germination and characterization of the inward potassium currents in *Arabidopsis* pollen grain protoplasts. Journal of Experimental Botany **52**, 1603–1614.

Farmer LM, Book AJ, Lee KH, Lin YL, Fu H, Vierstra RD. 2010. The RAD23 family provides an essential connection between the 26S proteasome and ubiquitylated proteins in *Arabidopsis*. The Plant Cell **22**, 124–142.

Fischer AH, Jacobson KA, Rose J, Zeller R. 2008. Hematoxylin and eosin staining of tissue and cell sections. Cold Spring Harbor Protocols **10**, 4986.

Haase SB, Wittenberg C. 2014. Topology and control of the cell-cycle-regulated transcriptional circuitry. Genetics **196**, 65–90.

Hamazaki J, Hirayama S, Murata S. 2015. Redundant roles of Rpn10 and Rpn13 in recognition of ubiquitinated proteins and cellular homeostasis. PLoS Genetics **11**, e1005401.

Hänzelmann P, Stingele J, Hofmann K, Schindelin H, Raasi S. 2010. The yeast E4 ubiquitin ligase Ufd2 interacts with the ubiquitin-like domains of Rad23 and Dsk2 via a novel and distinct ubiquitin-like binding domain. The Journal of Biological Chemistry **285**, 20390–20398.

Hirano H, Shinmyo A, Sekine M. 2011. Both negative and positive G1 cell cycle regulators undergo proteasome-dependent degradation during sucrose starvation in *Arabidopsis*. Plant Signaling & Behavior **6**, 1394–1396.

Isasa M, Katz EJ, Kim W, Yugo V, González S, Kirkpatrick DS, Thomson TM, Finley D, Gygi SP, Crosas B. 2010. Monoubiquitination of RPN10 regulates substrate recruitment to the proteasome. Molecular Cell **38**, 733–745.

Jefferson RA, Burgess SM, Hirsh D. 1986. beta-Glucuronidase from *Escherichia coli* as a gene-fusion marker. Proceedings of the National Academy of Sciences, USA **83**, 8447–8451.

Kurepa J, Wang S, Li Y, Zaitlin D, Pierce AJ, Smalle JA. 2009. Loss of 26S proteasome function leads to increased cell size and decreased cell number in *Arabidopsis* shoot organs. Plant Physiology **150**, 178–189.

Lai J, Chen H, Teng K, *et al*. 2009. RKP, a RING finger E3 ligase induced by BSCTV C4 protein, affects geminivirus infection by regulation of the plant cell cycle. The Plant Journal **57**, 905–917.

Li CY, Liu XM, Qiang XN, *et al*. 2018. EBP1 nuclear accumulation negatively feeds back on FERONIA-mediated RALF1 signaling. PLoS Biology **16**, e2006340.

Liang RY, Chen L, Ko BT, Shen YH, Li YT, Chen BR, Lin KT, Madura K, Chuang SM. 2014. Rad23 interaction with the proteasome is regulated by phosphorylation of its ubiquitin-like (UbL) domain. Journal of Molecular Biology **426**, 4049–4060.

Liu H, Ma X, Han HN, Hao YJ, Zhang XS. 2016. AtPRMT5 regulates shoot regeneration through mediating histone H4R3 dimethylation on *KRPs* and Pre-mRNA splicing of RKP in *Arabidopsis*. Molecular Plant **9**, 1634–1646.

Liu J, Zhang Y, Qin G, *et al*. 2008. Targeted degradation of the cyclin-dependent kinase inhibitor ICK4/KRP6 by RING-type E3 ligases is essential for mitotic cell cycle progression during *Arabidopsis* gametogenesis. The Plant Cell **20**, 1538–1554.

Lowe ED, Hasan N, Trempe JF, Fonso L, Noble ME, Endicott JA, Johnson LN, Brown NR. 2006. Structures of the Dsk2 UBL and UBA domains and their complex. Acta Crystallographica **D62**, 177–188.

Medina B, Paraskevopoulos K, Boehringer J, Sznajder A, Robertson M, Endicott J, Gordon C. 2012. The ubiquitin-associated (UBA) 1 domain of Schizosaccharomyces pombe Rhp23 is essential for the recognition of ubiquitin-proteasome system substrates both in vitro and in vivo. The Journal of Biological Chemistry **287**, 42344–42351.

Mueller JP, Smerdon MJ. 1996. Rad23 is required for transcription-coupled repair and efficient overall repair in *Saccharomyces cerevisiae*. Molecular and Cellular Biology **16**, 2361–2368.

Park SK, Howden R, Twell D. 1998. The *Arabidopsis thaliana* gametophytic mutation *gemini pollen1* disrupts microspore polarity, division asymmetry and pollen cell fate. Development **125**, 3789–3799.

Patton EE, Willems AR, Sa D, Kuras L, Thomas D, Craig KL, Tyers M. 1998. Cdc53 is a scaffold protein for multiple Cdc34/Skp1/F-box protein complexes that regulate cell division and methionine biosynthesis in yeast. Genes & Development **12**, 692–705.

Peng J, Yu D, Wang L, Xie M, Yuan C, Wang Y, Tang D, Zhao X, Liu X. 2012. *Arabidopsis* F-box gene *FOA1* involved in ABA signaling. Science China Life Sciences **55**, 497–506.

Ren H, Santner A, del Pozo JC, Murray JA, Estelle M. 2008. Degradation of the cyclin-dependent kinase inhibitor KRP1 is regulated by two different ubiquitin E3 ligases. The Plant Journal **53**, 705–716.

Renaud E, Miccoli L, Zacal N, Biard DS, Craescu CT, Rainbow AJ, Angulo JF. 2011. Differential contribution of XPC, RAD23A, RAD23B and CENTRIN 2 to the UV-response in human cells. DNA Repair **10**, 835–847.

Shen H, Moon J, Huq E. 2005. PIF1 is regulated by light-mediated degradation through the ubiquitin-26S proteasome pathway to optimize photomorphogenesis of seedlings in *Arabidopsis*. The Plant Journal **44**, 1023–1035.

Smalle J, Kurepa J, Yang P, Emborg TJ, Babiychuk E, Kushnir S, Vierstra RD. 2003. The pleiotropic role of the 26S proteasome subunit RPN10 in *Arabidopsis* growth and development supports a substrate-specific function in abscisic acid signaling. The Plant Cell **15**, 965–980.

Vieira P, de Almeida Engler J. 2017. Plant cyclin-dependent kinase inhibitors of the KRP family: potent inhibitors of root-knot nematode feeding sites in plant roots. Frontiers in Plant Science **8**, 1514–1523.

Weinl C, Marquardt S, Kuijt SJ, Nowack MK, Jakoby MJ, Hülskamp M, Schnittger A. 2005. Novel functions of plant cyclin-dependent kinase inhibitors, ICK1/KRP1, can act non-cell-autonomously and inhibit entry into mitosis. The Plant Cell **17**, 1704–1722.

Zhang J, Guo X, Li X, Xiang F, Zhou B, Yu D, Tang D, Liu X. 2012*a*. The genetic and physiological analysis of late-flowering phenotype of T-DNA insertion mutants of *AtCAL1* and *AtCAL2* in *Arabidopsis*. Molecular Biology Reports **39**, 1527–1535.

Zhang Y, Zhang M, Wu J, Lei G, Li H. 2012*b*. Transcriptional regulation of the Ufm1 conjugation system in response to disturbance of the endoplasmic reticulum homeostasis and inhibition of vesicle trafficking. PLoS ONE **7**, e48587–e48598.